Electronic supplementary information (ESI)

Controlled synthesis of $Co_xMn_{3-x}O_4$ nanoparticles with tunable composition and size for high performance lithium-ion batteries

Xiaoshi Hu, Chao Li, Xiaobing Lou, Xiaojing Yan, Yanqun Ning, Qun Chen, and Bingwen Hu,*

School of Physics and Materials Science, Shanghai Key Laboratory of Magnetic Resonance, East China Normal University, Shanghai 200062, PR China. E-mail: bwhu@phy.ecnu.edu.cn.

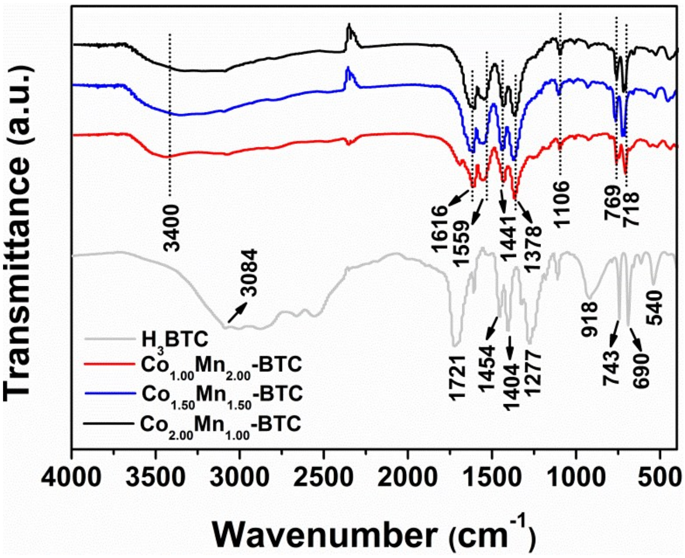

Fig. S1 IR spectrum of H_3BTC (the starting material) and Co_xMn_{3-x}-BTCs. It is observed that in the FTIR spectrum of Co_xMn_{3-x}-BTCs, the characteristic bands (ν_{OH}, 3084 cm^{-1}; $\nu_{C=O}$, 1721 cm^{-1}; $\delta_{C=O}$, 540 cm^{-1}) of the nonionized carboxyl groups of 1,3,5-BTC disappear, and new bands appear in the regions 1616−1559 cm^{-1} (asymmetric stretching vibrations of $-COO^-$), 1441−1378 cm^{-1} (symmetric stretching vibrations of $-COO^-$), and at 769 cm^{-1} (ring-out-of-plane vibration of the 1,3,5-substituted benzene core of the linker molecules), which suggests that the metal ions have been coordinated with the 1,3,5-BTC ligands successfully. A similar kind of observation has been made for manganese 1,3,5-benzenetricarboxylate MOF. [1]

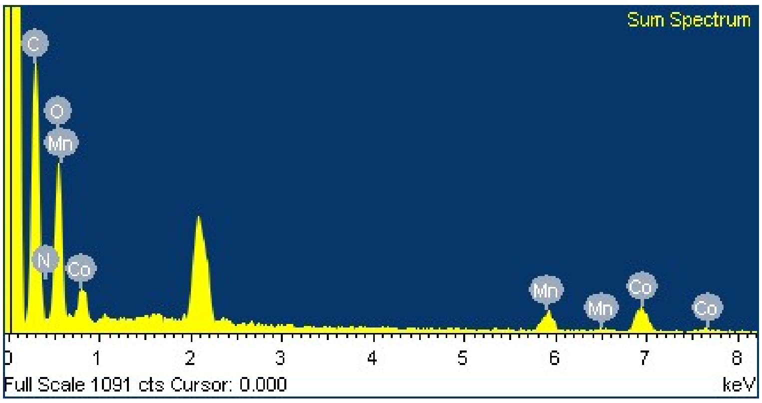

Fig.S2 EDX spectra of Co_xMn_{3-x}-BTC compound with x=2.00 on selected area. The sample was composed of Co, Mn, O and C.

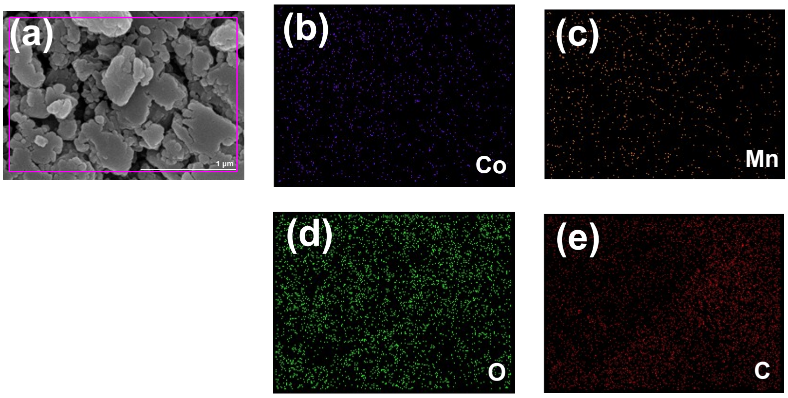

Fig.S3 (a) SEM Image and (b-e) EDX mapping images of the Co_xMn_{3-x}-BTC compound with x=2.00 on selected area. The homogeneous distribution of Co and Mn elements in the whole sample indicated that the reaction of 1,3,5-benzenetricarboxylic acid ligand with Co and Mn ions could result in bimetallic CPs as pure phase rather than a mixture of two homometallic CPs.

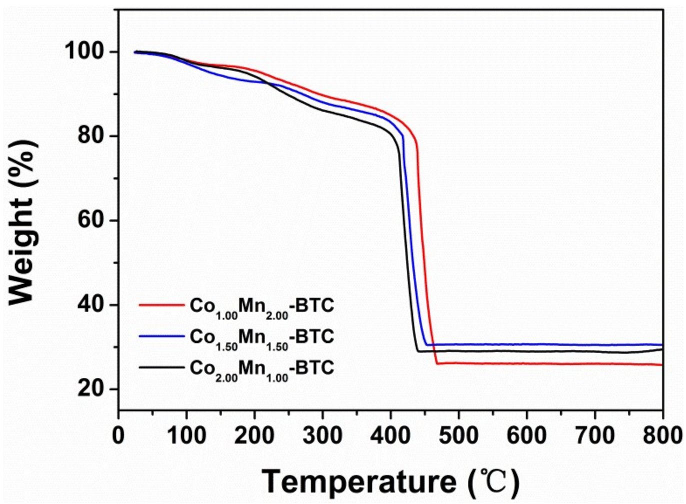

Fig. S4 TG analysis curves of the as-synthesized Co_xMn_{3-x}-BTCs under air flow.

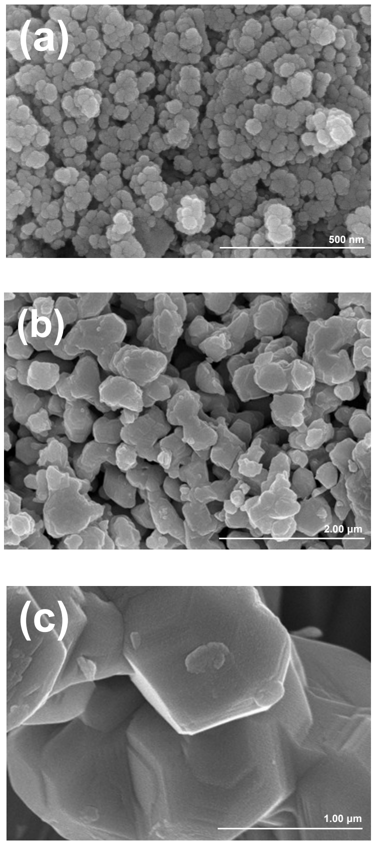

Fig. S5 SEM images of $MnCo_2O_4$ particles for different calcinating temperatures: (a) 400 ℃ ($MnCo_2O_4$-400C), (b) 600 ℃ ($MnCo_2O_4$-600C), and (c) 800 ℃ ($MnCo_2O_4$-800C).

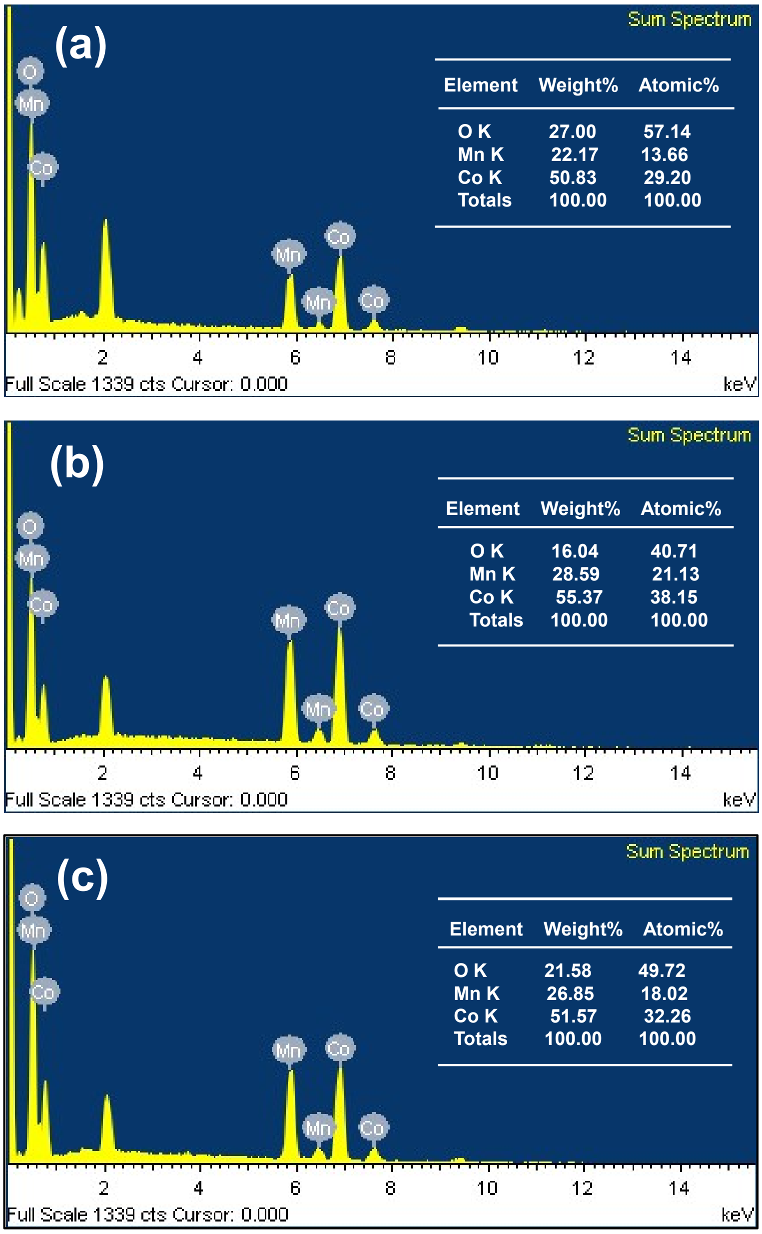

Fig. S6 EDX spectra and corresponding element analysis of (a) $MnCo_2O_4$-400C, (b) $MnCo_2O_4$-600C, and (c) $MnCo_2O_4$-800C.

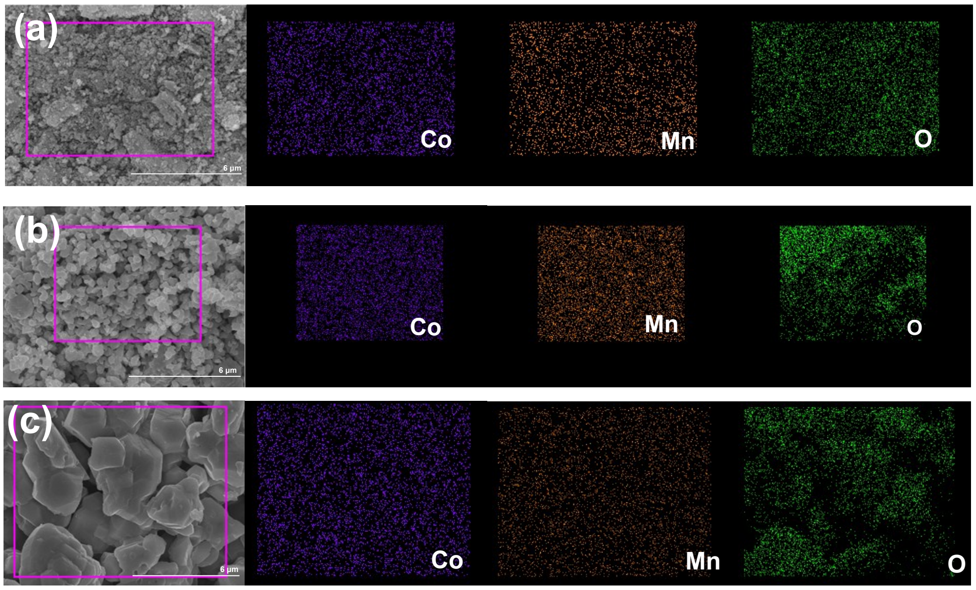

Fig .S7 EDX mapping images for a selected region of (a) $MnCo_2O_4$-400C, (b) $MnCo_2O_4$-600C, and (c) $MnCo_2O_4$-800C.

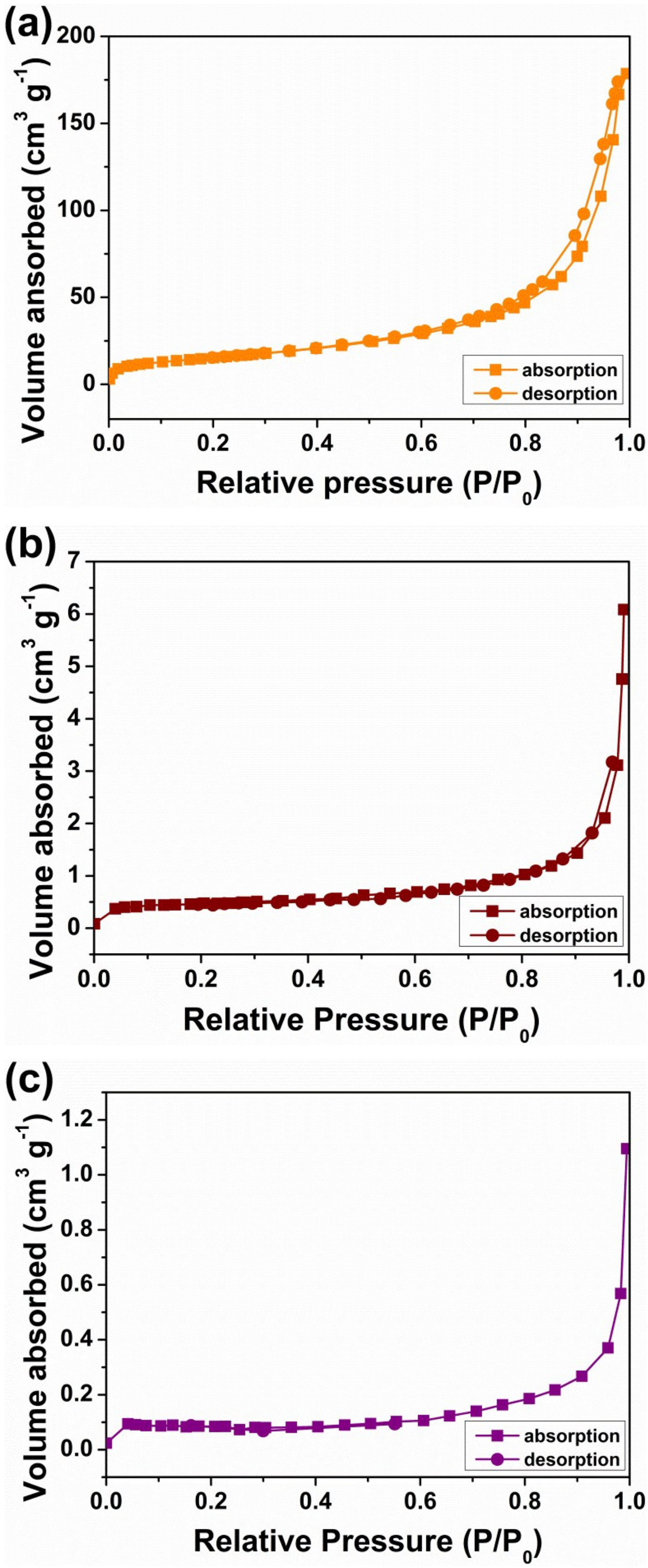

Fig. S8 Nitrogen adsorption/desorption isotherms of (a) $MnCo_2O_4$-400C, (b) $MnCo_2O_4$-600C, and (c) $MnCo_2O_4$-800C.

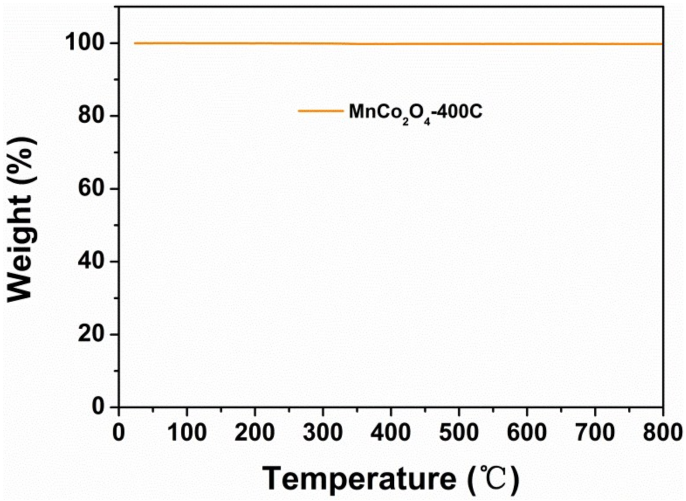

Fig. S9 TGA curve of $MnCo_2O_4$-400C under air flow.

References

1 S. Maiti, A. Pramanik, U. Manju and S. Mahanty, ACS Appl. Mater. Interfaces, 2015, 7, 16357 - 16363.